Registration of an on-axis see-through head-mounted display and camera system

Gang Luo
Harvard Medical School
Schepens Eye Research Institute
Boston, Massachusetts 02114
E-mail: gangluo@vision.eri.harvard.edu

Noa Rensing
Evan Weststrate
MicroOptical Engineering Corporation
Westwood, Massachusetts 02090

Eli Peli, MEMBER SPIE
Harvard Medical School
Schepens Eye Research Institute
Boston, Massachusetts 02114

Abstract. An optical see-through head-mounted display (HMD) system integrating a miniature camera that is aligned with the user's pupil is developed and tested. Such an HMD system has a potential value in many augmented reality applications, in which registration of the virtual display to the real scene is one of the critical aspects. The camera alignment to the user's pupil results in a simple yet accurate calibration and a low registration error across a wide range of depth. In reality, a small camera-eye misalignment may still occur in such a system due to the inevitable variations of HMD wearing position with respect to the eye. The effects of such errors are measured. Calculation further shows that the registration error as a function of viewing distance behaves nearly the same for different virtual image distances, except for a shift. The impact of prismatic effect of the display lens on registration is also discussed. © *2005 Society of Photo-Optical Instrumentation Engineers.*
[DOI: 10.1117/1.1839231]

1 Introduction

Augmented reality (AR) technology, in which a virtual display is combined with a veridical view of the environment, has potential value in numerous areas such as medicine,[1–5] manufacturing,[6] visualization,[7,8] and communication.[9] Since the early 1990s, AR technology has progressed rapidly, yet few commercial products have become available. Registration error between the displayed augmenting information and the view of the real world has been cited as a major obstacle to AR.[10] To match a virtual display to the real world, a user's viewpoint in the real world must be known. This is currently done in one of two ways. First, a position tracking system can measure the position of a user's eye with respect to the real world,[11–15] and second, a head-mounted video camera can capture what a user sees (video-based tracking).[8,9,16–19] Since generally neither the position-tracking sensor nor the video camera is coincident with the user's eye, parallax calibration is required in both approaches to transform the coordinates of sensors (tracking sensor or video camera) to those of the user's eye. Such calibration would not be necessary if a sensor was placed right on a user's eye to result in a very small parallax. While such an eye-tracking technology (scleral search coil) is available,[20] to our knowledge, it has not been applied to AR, possibly because it is extremely uncomfortable.

Video-based tracking techniques for AR systems have been widely adopted because video cameras offer very accurate yet economical and compact tracking solutions. Such systems were used in applications with known and prepared environments,[6,8,9] extended unprepared environments,[18] and also in combination with position tracking sensors in mobile applications.[21] AR systems that use video-based tracking techniques usually depend on fiducial marks or template targets in the real world. They align the virtual display to the real world by detecting those features.[19] In many of these systems, the sensing cameras are not aligned with the user's eye, and parallax results. The impact of parallax on the registration varies for different object distances; hence complicated camera calibration[18,19] or perspective projection analysis[16,17] is usually required.

Video see-through AR systems use a head-mounted display (HMD) that is optically opaque with respect to the real world and present an image of the real world acquired by a head-mounted camera that is combined with a virtual or graphic image. The parallax issue affects those video see-through AR systems where the cameras (virtual eyes) are displaced from the users' eyes.[14] If the camera is aligned with the user's eye, the camera view always matches what the user is seeing as long as the parameters of the camera (magnification and alignment) are appropriate. Thus, the parallax effects could be eliminated, and simple calibration and accurate registration can be achieved. This is therefore the aim in the development of aligned systems for video see-through HMDs.[4,22–24]

We developed and tested an on-axis optical see-through AR system in which a camera is aligned with the viewer's eye. One potential application of such a system is a vision rehabilitation device that applies wide-band enhancement to improve the visibility of the real world for patients with central field loss.[25,26] In this application, a 1:1-size bright edge contour of the real world needs to be precisely superimposed over the patients' natural view (Fig. 1). Because accurate registration is essential in such an application, the on-axis design is critical. In addition, the same design can also be used in other optical see-through as well as video see-through AR systems requiring low registration error across a large depth range.
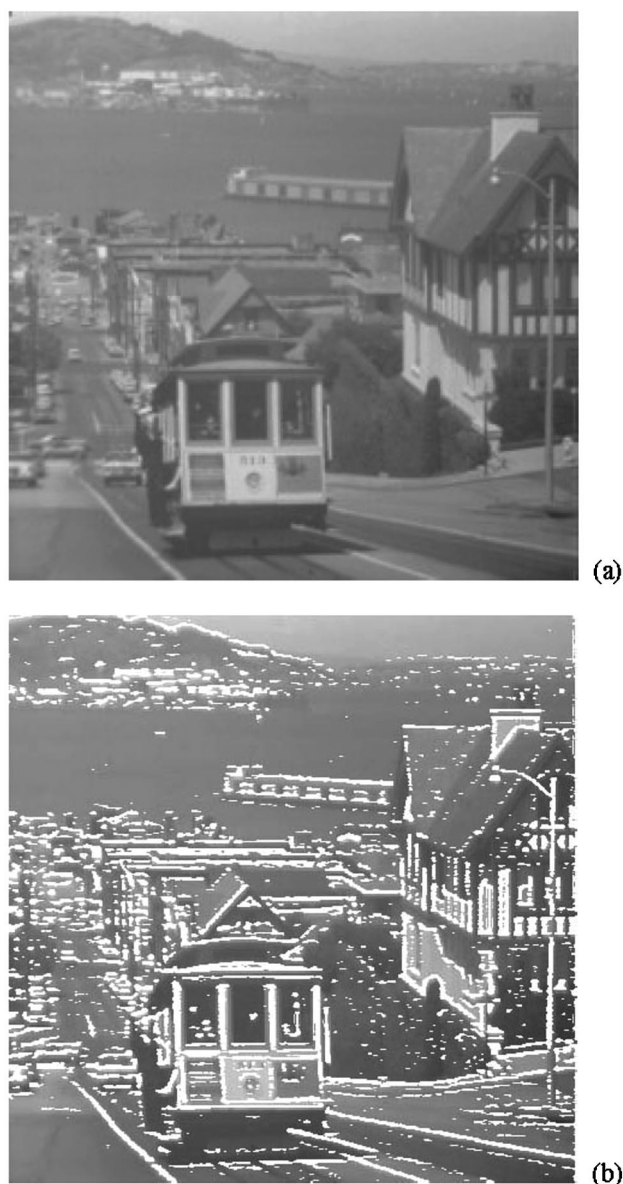
Fig. 1 Illustration of the wide-band enhancement effect: (a) original image (representing the natural view through the display; (b) its edge image (obtained with a DigiVision edge detector used in this study) superimposed over the original image to simulate the user's view.

2 Integrated HMD-Camera System Design

Based on the original design of the in-spectacle-lens HMD of the MicroOptical Corporation[27] (Westwood, Massachusetts) we developed a see-through HMD, which we call the on-axis see-through head-mounted display and camera system. This system consists of an optical see-through HMD (field of view=15 deg, nominal focus at 2 m), a miniature video camera, and an image processor. The miniature camera (Panasonic GP-KS462 with ±0.3 diopter depth of focus) is integrated into the HMD optics to be aligned to the viewer's pupil. A customized image processing system (DigiVision Incorporated, San Diego, California) performs edge detection as well as electronic adjustments of video image size and position to compensate for minor manufac-

turing errors in the prototype. The edge detection was developed specifically for the purpose of wide-band enhancement for patients with reduced visual resolution.[25] In this work, we made use of the edge detector to evaluate the registration error.

The image processing system carries out real-time video signal processing at a rate of 30 frames/sec with a 73-μs delay (a little more than one scan line of NTSC signal). Thus, other than the image processing, most of the delay through the whole system is associated with the camera and the interlacing video format. When a user moves his/her head with respect to the real object being viewed, an observable misregistration may occur, depending on the speed. However, we expect that the visually impaired patients might have higher tolerance to the dynamic misregistration than normal-vision users due to their poor spatial resolution. In any case, the misregistration is only fleeting, and once head position is stabilized, the registration is regained.

The same system can also be used as a visual field expansion aid for patients with peripheral field loss.[28] In that application, a minified edge contour of the real scene (from a wide-field camera) is superimposed over the patients' natural but severely restricted field of view (FOV) (typically 10 deg in diameter or less). For example, with a minification factor of 4.0, the patient's instantaneous field is expanded to 40 deg in the contour view. This device also needs to function over a wide range of viewing distance. Although the requirement for registration is relatively lower in this case due to the minification, reasonable registration is still needed to aid patients in determining the real positions of objects when using the minified view.[29]

A schematic of the design of the system's optics is shown in Fig. 2, and a picture of the integrated HMD-camera system is shown in Fig. 3. Part of the light paths for both the camera and the display overlap in the spectacle lens. For clarity, Fig. 2(a) illustrates only the display's optical path and the components pertinent to the display. Light from an illuminator passes through the LCD and enters the spectacle lens. The light is linear polarized light and it is selected to pass through a polarizing beamsplitter (PBS). The polarized light propagates through a quarter-wave plate (QWP) and is reflected from a concave mirror that magnifies the image. The reflected light passes again through the QWP. Having passed twice through the QWP, it becomes polarized in the orthogonal direction and is therefore reflected from the PBS to the eye. This approach is the basis for MicroOptical's integrated eyewear display lenses.[27]

The camera optics share some of the same optical elements with the display, but in a different manner. Figure 2(b) illustrates that light from the ambient scene enters the spectacle lens through a polarizer and is reflected by the PBS inside the spectacle lens. A second PBS reflects the polarized light toward the camera lens and sensor. Thus, the camera views the real world in a periscope fashion. By using this design, the camera can be coaxially aligned with the eye to avoid parallax.

Figure 2(c) shows the optical path for the combined display and camera system. This is the actual design applied in the prototype unit shown in Fig. 3. Note that the display and camera use orthogonal polarizations, and thus, each can
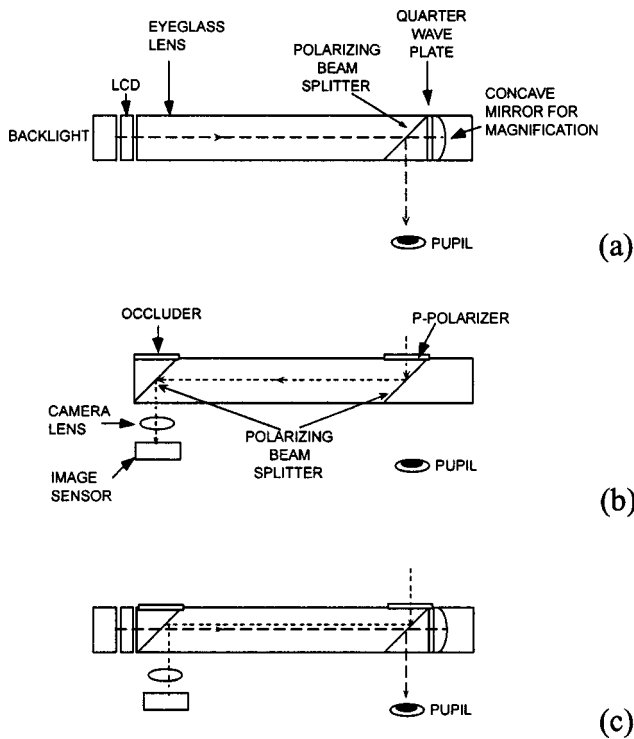
Fig. 2 A schematic illustration of the on-axis HMD-camera system design, viewed from above: (a) display system only integrated into a spectacle lens; (b) camera system only integrated into a spectacle lens; (c) camera and display systems combined in the same spectacle lens.

have independent optical paths within the same spectacle lens.

While the camera's entrance pupil is coaxial with the user's pupil, its optical path is about 20 mm longer than that of the user's pupil. (The exact amount depends on the face form of the user.) This on-axis disparity causes an effect of displacing images (environment) outward. Although such a sensory rearrangement may have negative effect on hand-eye coordination, generally, adaptation may be expected.[30] On the other hand, such a small displacement may be ignored for most applications, where the working distance is much greater than 20 mm. It is possible
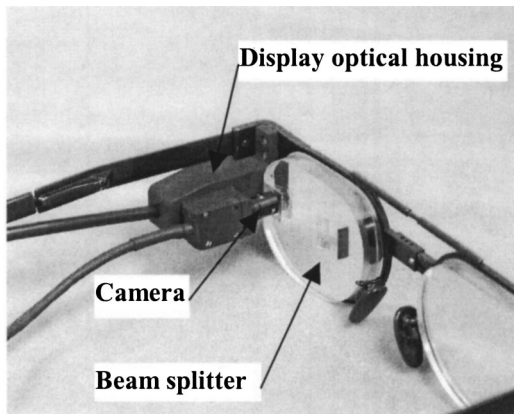
Fig. 3 The optical see-through head-mounted display with integrated on-axis camera.
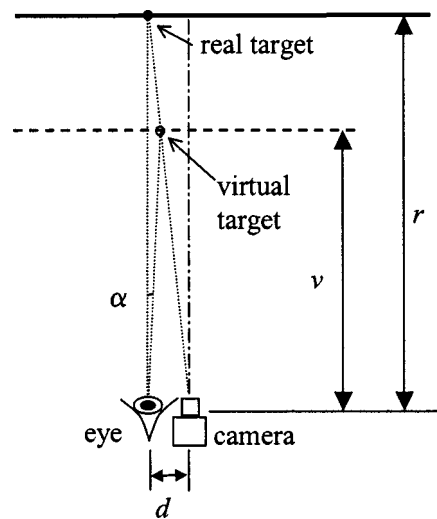
Fig. 4 A parallax and difference between the virtual display plane and the real target plane cause a registration error. Here, r is the distance from eye to real target, v is the distance of the virtual display plane, d is the deviation of the HMD-camera system from the user's pupil, and α denotes angular registration error.

to completely eliminate this disparity by moving the spectacle lens 20 mm outward, as designed in Refs. 4, 22, 23, and 24, but this would significantly increase the size of the HMD and compromise its ergonomic design and aesthetic appearance.

3 Parallax and Registration Error

Besides the parallax mentioned earlier, the variable difference between the image plane of the virtual display and the plane of the real object is also a factor that affects the registration for AR systems that operate over a wide range of real-world depth. As illustrated in Fig. 4, assuming that the HMD-camera system is initially aligned to the user's eye and the registration error is zero, a shift of the HMD-camera system with respect to the user's pupil may cause a registration error whenever the virtual display plane does not coincide with the real-world plane where a target is presented. Ignoring optical distortions of the camera, the angular registration error α is

$$\alpha = \tan^{-1}\left(\frac{r-v}{rv} \cdot d\right), \qquad (1)$$

where r and v are the distance from the real-world plane and the virtual display plane to the user's eye, respectively, and d is the deviation of the HMD-camera system from the user's pupil.

An experimental setup, as illustrated in Fig. 5, was used to measure the registration error of the aligned HMD-camera system. A round target was displayed sequentially at different locations on a computer screen. A normally-sighted subject wearing the HMD was able to see the real target through the optical see-through display. The video image from the camera was processed into an edge contour image and presented as a circle on the HMD. The subject could see the circular edge contour of the target on the virtual display and the real target simultaneously. The sub-
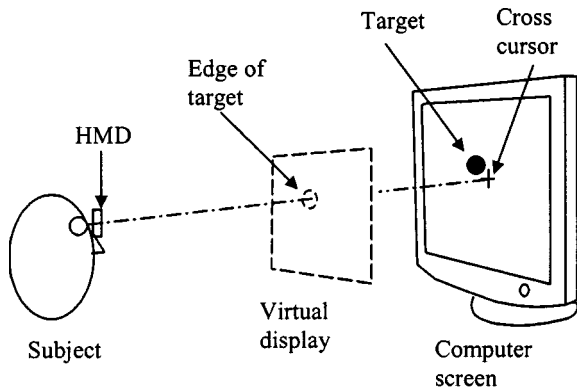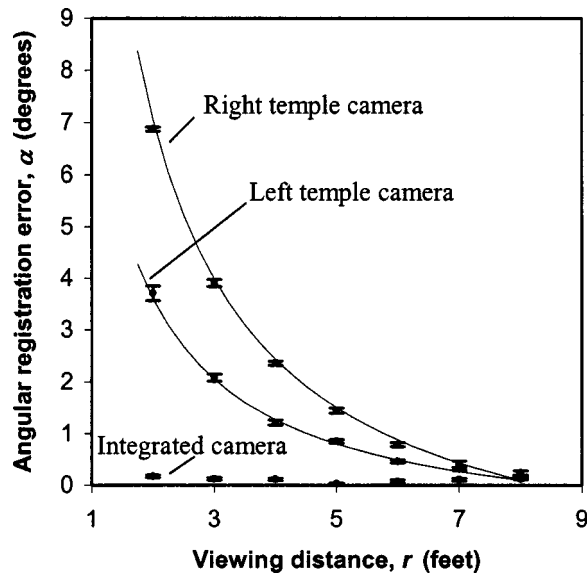
Fig. 5 Schematic diagram of the experimental setup used for measurement of registration error. The subjects observed the desktop computer screen through the HMD. The image of the round target on the screen captured by a head-mounted camera (not shown) was processed to provide a circular edge image displayed on the HMD and seen on the virtual screen. The subject controlled the position of the cross cursor on the screen to align it with the center of the circular edge contour on the virtual display. The distance between the cursor and the target on the computer screen is a measure of the misregistration.

Fig. 6 Averaged absolute value of registration errors of the integrated HMD-camera system measured at different viewing distances compared with the errors when the camera was mounted on the left and right temples, respectively. (The virtual display was in the left spectacle lens.) Error bars represent ±1 standard deviation of measurements. The curves are calculation results according to Eq. (1) for d of 50 and 100 mm, respectively.

ject was instructed to align a cross-shaped mouse cursor presented on the computer screen with the center of the circular edge contour presented on the virtual display. The target on the computer screen was green and its edge contour on the virtual display was white, which allowed the subject to distinguish them from each other when they overlapped. The mouse cursor consisting of thin crosshairs was not detected by the camera and edge detector but was easily seen through the HMD. The subject clicked a mouse button to record the position of the cursor on the computer screen when she/he aligned the edge contour and cross cursor. The registration error was measured by comparing the positions of the real target and that of the mouse cursor.

As human observers are involved in the evaluation of registration, it is possible that different testers would yield different results due to different hand-eye coordination abilities. An approach has been adopted to replace the human eye with a video camera in other registration evaluation studies.[13] However, we found that most observers' cursor pointing capabilities were well beyond the resolution and registration performance that our system can achieve.

Three subjects with normal vision were instructed to align the mouse cursor with 25 targets presented on a desktop monitor (without wearing the HMD). Testing was done at distances that varied from 2 to 8 feet. Their averaged absolute alignment errors were 0.0044, 0.0045, and 0.0057 deg, respectively. It is seen that these values are much smaller than the registration errors we attempted to measure here.

Because the prototype system was constructed using some off-the-shelf components, there were manufacturing inaccuracies in magnification, tilt, and position in the prototype. As a part of the final calibration and setting, the HMD magnification was adjusted by an operator (whose alignment error was 0.0044 deg in the hand-eye coordination testing). The same experimental setup was used for these adjustments as that illustrated in Fig. 5. A 5×5 target array, which, at a distance of 2 feet to the operator's eye

spanned 8×8 deg, was presented on the computer monitor. The operator wearing the HMD-camera system recorded the positions of the target contours, as described before. As it was difficult to judge the small misalignment visually, the system was adjusted as described later. The measured array of target contours was fitted to the real target array by using a least squares data fitting algorithm, in which two shift coefficients (in x and y directions), one size coefficient (for both x and y), and a rotation coefficient were computed. The magnification and rotation errors are reflected by the size and rotation coefficients, respectively. The rotation error of the camera was corrected by mechanical adjustment, and the electronic zoom function of the image processor was used to compensate for the magnification error of the system. After a few iterations of careful adjustments, recordings, and fitting calculations, the size and rotation coefficients obtained by the fitting calculation converged to 1.03× and 0.03 deg, respectively, which indicates that there was a 3% magnification error and a 0.03-deg rotation error remaining in the prototype system.

Following the magnification and rotation adjustments, experiments for registration evaluation were carried out at different viewing distances by a human subject. At each distance, a round target was presented at 25 different positions, and the recordings at these 25 positions were used to estimate the registration error for that viewing distance. Registration errors were calculated by averaging the absolute distance between each real target and its displayed edge image, and then converted to viewing angle.

Figure 6 shows the registration errors measured at different viewing distances. Error bars represent standard deviation of the measurements, which include random measurement error (negligible effect) and systemic errors, such as residual magnification error, residual rotation error, and

optical distortions in the camera and display optics. Similar measurements also were also carried out using a different miniature camera (Marshall lipstick camera V-3214) mounted on the temple on either side of the HMD (the virtual display was mounted in the left spectacle lens). An experiment with each camera took between 15 to 20 min. The measurements were made at viewing distances ranging from 2 to 8 feet at 1-foot increments. For each camera position, the registration was first adjusted at a distance of 8 feet to be reasonably good (the registration error turned out to be about 0.1 deg after analysis) using both electronic shifting via the image processor and mechanical camera adjustment. While keeping the same adjustments, the computer screen was moved closer to the subject and the measurements were made at different distances. As shown in Fig. 6, the registration error remains almost constant across all distances with our on-axis camera aligned to the subject's pupil. However, with a camera mounted on one of the temples, the angular registration error increases rapidly when the viewing distance decreases. While the registration errors for the on-axis camera and the left temple camera were about the same at 8 feet, the error of the on-axis camera at 2 feet distance was only about 5% of that of the left temple camera. The registration was even worse for the right temple camera mount, as anticipated.

In Fig. 6, two curves calculated according to Eq. (1) are also shown for the temple-mounted cameras. In calculation, the virtual display distance v was a nominal 6 feet, and the deviation of the HMD-camera system from pupil d was 50 mm for the camera mounted by the left temple and 100 mm for the camera mounted by the right temple, which were directly measured from the subject's pupil to the camera lens. For the purpose of comparison, the calculated curves were offset to make the calculated registration error 0.1 deg at an 8-foot viewing distance. It can be seen that the calculated results match the recorded data well.

Ideally, manufacturing errors can be reduced adequately and optical distortions can be carefully compensated to result in an aligned on-axis HMD-camera system free of registration error at all distances. In practice, however, misregistration may still occur due to variation of the HMD position with respect to a user's eye. A user may wear an HMD in slightly different positions from session to session, and different users are likely to have different viewpoints because of variations of users' head form, frame adjustment, and uncertainty of placement of the frame on the head. These variations may cause an unpredictable change of alignment. A pattern of different registration errors of different users was demonstrated in Ref. 31. Therefore, we further studied the registration error of the integrated HMD-camera system caused by such unpredictable yet small deviations.

The recorded data for the on-axis camera were fed into a least square fitting program to derive the HMD deviation, using Eq. (1) as the fitting model. Figure 7 shows one fitting calculation, in which only the data of vertical registration error (directional) were used to solve for the vertical HMD deviation. Note the data in Fig. 6 are all absolute values and the data in Fig. 7 are directional. The use of directional data is for solving the specific direction of the HMD deviation. The computed parameters in the fitting calculation were virtual display distance v and deviation of
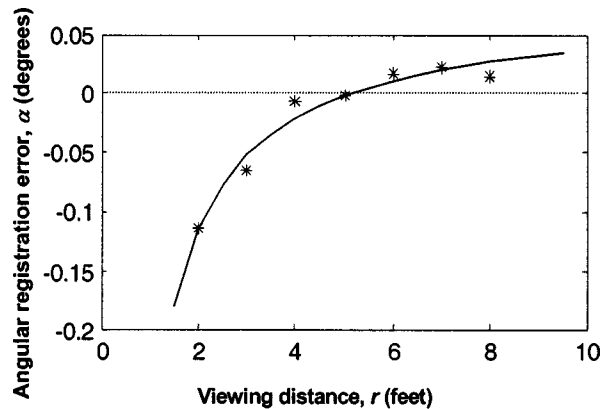

Fig. 7 Measurement of registration error due to deviation of the HMD on the head and a fitted curve using Eq. (1). The zero crossing point of the fitted curve around 5-ft distance suggests that the virtual display distance was about 5 ft (as compared to the nominal design of 6 ft).

HMD d. After fitting, the returned parameter v was 5.14 feet, which means the estimated virtual display distance was 5.14 feet, and the returned parameter d was 2.01 mm, which means the estimated vertical deviation of the HMD was 2.01 mm. The result suggests that the constant registration error of the aligned HMD-camera system was still due to a minor parallax. Without a precision adjustment, this kind of unseen parallax is very likely to exist in any HMD wearing.

The method of fitting of directional registration error can be used in a delicate adjustment to diminish the deviation. By multiple iterations of measurement, fitting, and adjustment, guided by fitting results, a near zero-deviation setup can be achieved.

Figure 8 shows calculated results [Eq. (1)] of registration error due to a 2-mm HMD deviation across a depth range from 1 to 12 feet. Calculations for different virtual
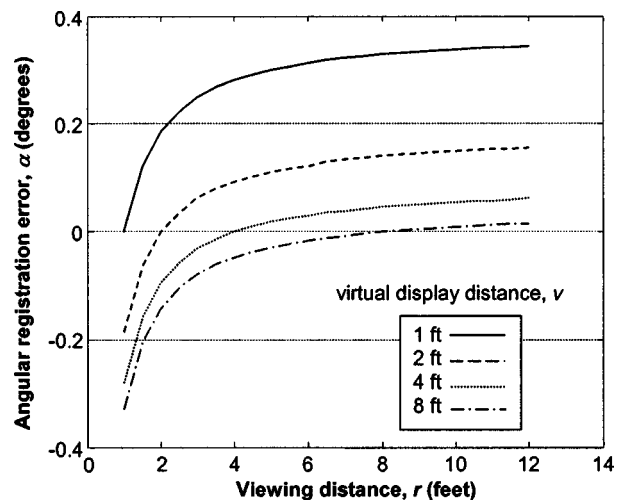

Fig. 8 Calculated results of directional registration errors due to 2-mm off-axis parallax. Results for different virtual display distance (1, 2, 4, and 8 feet) across a depth range from 1 to 12 feet are shown. It can be seen that the variations of registration with viewing distance for different virtual display distances behave nearly the same. The offsets between the various curves can be compensated for by lateral shift electronically.

display distances (1, 2, 4, and 8 feet) are shown. Clearly, the registration varies with depth more significantly when targets are at small distances. For example, the registration varies as much as 0.24 deg within the range of viewing distances from 1 to 3 feet, while for the much wider range from 3 feet to infinity, the registration varies only by 0.12 deg. Therefore, deviation of the HMD (parallax) is a critical factor for those applications with short viewing distances (within arms' reach).

It is also apparent that for different virtual display distances, the registration error as a function of depth behaves approximately the same. This actually applies to all AR systems, irrespective of the magnitude of the parallax. While Fig. 8 shows that the registration error for a 1-foot virtual display distance is higher than that for larger virtual display distances, it does not suggest an HMD with a shorter display distance will have worse registration. The registration offset may be adjusted by shifting the virtual display. In any case, the virtual display distance should be designed to be as close to the real target as possible. This will maximize the likelihood that both the real targets and the virtual display are in focus at the same time, and an accommodation conflict is avoided.

In addition to the parallax effect, the prismatic effect of the display magnifying lens may also cause registration error when an HMD is offset from the user's eye. If the virtual display distance of an HMD is short, the prismatic effect may be significant.[32] Determined approximately by the Prentice rule, the prismatic effect is

$$\Delta = \frac{d[\text{cm}]}{v[\text{meter}]}, \qquad (2)$$

where Δ is in prism diopters (1 prism diopter=10 mrad), d is the deviation of the HMD center from the user's pupil center in centimeters, and v is the virtual display distance in meters.[32] For instance, the prismatic effect causes a registration error of 0.37 deg in an HMD with a virtual display distance of 1 foot when the deviation of the HMD from the user's eye is 2 mm. The registration error caused by the prismatic effect is independent of the target distance. Therefore, it is possible to correct it by electronically shifting the display. On the other hand, this kind of registration error can be reduced by proper design. In principle, a long virtual display distance will diminish the prismatic effect.[32]

Figure 9 shows an example of registration with the on-axis HMD-camera system. The picture was captured with a digital camera looking through the HMD. Five identical white bars (25 mm long) printed on papers were placed at 3, 4, 5, 6, and 7 feet from the HMD system. For the purpose of clear illustration, the environment and the edge detector were set up so that only the white bars' edge contours were shown in the display. The registration was vertically offset by electronically shifting the image to allow the real white bars and their edge images to be seen simultaneously. Five identical gauges are depicted next to the bar pairs in the picture to help the readers compare the registrations at different distances. As can be seen, the registration was very consistent from 3 to 7 feet. If the display image was electronically shifted up, the contours would coincide with the bars. The registration difference between the 3 and 7 feet distances is estimated from the picture to be about 0.07 deg.
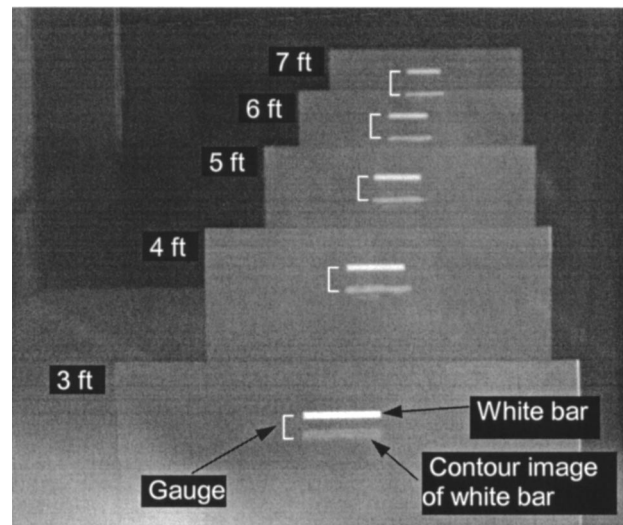
Fig. 9 An example of consistent registration performance across a wide range of distances. Five identical white bars were placed at 3, 4, 5, 6, and 7 feet from the HMD system. The registration was electronically shifted down to provide clear visibility of the real objects and the virtual edge images simultaneously. This picture was captured with a digital camera aiming through the HMD. Five identical gauges depicted next to the white bars show the registration was consistent from 3 to 7 feet.

4 Conclusion

Most AR systems require that complicated calibration procedures be solved for the position of camera relative to the user's pupil. In the case of the on-axis HMD-camera system presented here, it is possible that the calibration may not be needed. Like a "plug-and-play" device, such a system may stay calibrated from session to session and from person to person, offering low registration error, provided that the necessary frame adjustment is performed. The registration errors are very low across a wide depth range, which makes the system suitable for applications with wide-ranging environments. The novel integration technique we developed offers a light, compact, and aesthetic see-through HMD-camera system. This makes this approach to an AR appealing for future applications. Uncertainty in the position of the HMD relative to the eye remains the major cause of registration error in an on-axis HMD. The impact of the deviation of the HMD becomes great when object distance is short. For those applications where this variation of registration may exceed the registration tolerance, adjustment of fitting or calibration by the user might be needed before each use. If fiducial marks are provided and a brief camera calibration is performed, the on-axis HMD-camera system would still result in a better registration, despite the inevitable camera-eye misalignment.

References

1. M. Rosenthal et al., "Augmented reality guidance for needle biopsies: An initial randomized, controlled trial in phantoms," *Med. Image Anal* **6**(3), 313–320 (2002).
2. S. L. Tang, K. Kwoh, M. Y. Two, N. W. Sing, and K. V. Ling, "Augmented reality systems for medical applications," *IEEE Eng. Med. Biol. Mag.* **17**(3), 49–58 (1998).
3. R. J. Gove, "System and method for simultaneously viewing a scene and an obscured object," United States Patent No. 5,491,510 (1996).
4. H. Fuchs et al., "Augmented reality visualization for laparoscopic surgery," in *Proc. Med. Image Computing Computer-Assisted Intervention (MICCAI) '98* Lecture Notes in Computer Science 1496, 934–943 (1998).
5. J. P. Rolland and H. Fuchs, "Optical versus video see-through head-mounted displays in medical visualization," *Presence: Teleoperators and Virtual Environments* **9**(3), 287–309 (2000).
6. D. Sims, "New realities in aircraft design and manufacture," *IEEE Comput. Graphics Appl.* **14**(2), 91 (1994).
7. S. K. Feiner, A. C. Webster, T. E. Krueger III, B. MacIntyre, and E. J. Keller, "Architectural anatomy," Presence **4**(3), 318–325 (1995).
8. M. Billinghurst, H. Kato, and I. Poupyrev, "The magicbook—moving seamlessly between reality and virtuality," *Computer Graphics Appl.* **21**(3), 2–4 (2001).
9. M. Billinghurst, "Real world teleconferencing," *IEEE Comput. Graphics Appl.* **22**(6), 11–13 (2002).
10. R. Azuma, "A survey of augmented reality," *Presence: Teleoperators and Virtual Environments* **6**(4), 355–385 (1997).
11. R. Azuma and G. Bishop, "Improving static and dynamic registration in an optical see-through HMD," *Proc. SIGGRAPH '94*, 197–204 (1994).
12. H. Hua, C. Gao, and N. Ahuja, "Calibration of a head-mounted projective display for augmented reality systems," *Proc. Intl. Symp. Mixed Augmented Reality, ISMAR 2002* Darmstadt, Germany, Sept. 30–Oct. 01 (2002), pp. 176–185.
13. M. Tuceryan, Y. Genc, and N. Navab, "Single point active alignment method (spaam) for optical see-through HMD calibration for augmented reality," *Presence: Teleoperators and Virtual Environments* **11**(3), 259–276 (2002).
14. M. Tuceryan et al., "Calibration requirements and procedures for augmented reality," *IEEE Trans. Vis. Comput. Graph.* **1**(3), 255–273 (1995).
15. M. Bajura and U. Neumann, "Dynamic registration correction in video-based augmented reality systems," *IEEE Comput. Graphics Appl.* **15**(5), 52–60 (1995).
16. K. Kutulakos and J. Vallino, "Calibration-free augmented reality," *IEEE Trans. Vis. Comput. Graph.* **4**(1), 1–20 (1998).
17. Y. Seo and K. S. Hong, "Calibration-free augmented reality in perspective," *IEEE Trans. Vis. Comput. Graph.* **6**(4), 346–359 (2000).
18. B. Jiang and U. Neumann, "Extendible tracking by line auto-calibration," *Proc. IEEE ACM Intl. Symp. Augmented Reality*, pp. 97–103 (2001).
19. M. Uenohara and T. Kanade, "Vision-based object registration for real-time image overlay," *Computters in Biology and Medicine* **25**(2), 249–260 (1995).
20. J. N. v. d. Geest and M. A. Frens, "Recording eye movements with video-oculography and scleral search coils: A direct comparison of two methods," *J. Neurosci. Methods* **114**(2), 185–195 (2002).
21. R. Azuma et al., "Tracking in unprepared environments for augmented reality systems," *Computers Graph.* **23**(6), 787–793 (1999).
22. E. K. Edwards, J. P. Rolland, and K. P. Keller, "Video see-through design for merging of real and virtual environments," *Proc. IEEE VRAIS '93*, Seattle, WA, pp. 223–233 (1993).
23. A. Takagi, S. Yamazaki, Y. Saito, and N. Taniguchi, "Development of a stereo video see-through HMD for AR systems," *Proc. ISAR*, pp. 68–77 (IEEE and ACM, 2000).
24. Y. Hadani, "Night-vision equipment," United States Patent No. 4,467,190 (1984).
25. E. Peli, "Wide-band image enhancement," U.S. Patent No. 6,611,618 (2003).
26. E. Peli, J. Kim, Y. Yitzhaky et al., "Wideband enhancement of television images for people with visual impairments," *J. Opt. Soc. Am. A* **21**(6), 937–950 (2004).
27. M. B. Spitzer et al., "Optical approaches to incorporation of displays within glasses," *J. Soc. Inf. Disp.* **6**, 211–212 (1998).
28. F. Vargas-Martin and E. Peli, "Augmented view for restricted visual field: Multiple device implementations," *Optom. Vision Sci.* **79**(11), 715–723 (2002).
29. G. Luo and E. Peli, "Kinematics of visual search by tunnel vision patients with augmented vision see-through HMD," *SID04 Digest*, pp. 1578–1581 (2004).
30. F. A. Biocca and J. P. Rolland, "Virtual eyes can rearrange your body: Adaptation to visual displacement in see-through, head-mounted displays," *Presence: Teleoperators Virtual Environments* **7**(3), 262–277 (1998).
31. E. McGarrity, Y. Gene, M. Tuceryan, C. Owen, and N. Navah. "A new system for online quantitative evaluation of optical see-through augmentation," *Proc. IEEE ACM Intl. Symp. Augmented Reality*, pp. 157–166 (2001).
32. E. Peli, "Optometric and perceptual issues with head-mounted display (HMD)," in *Visual Instrumentation: Optical Design and Engineering Principles*, P. Mouroulis, Ed., pp. 205–276, McGraw-Hill, New York (1999).

Gang Luo received his PhD in instrumentation from Chongqing University, China, in 1997. Then he studied optical information processing and digital image processing of color photography from 1997 to 1999 as a postdoctoral fellow at Nankai University, China. He was a research fellow from 1999 to 2001 at Nanyang Technological University, Singapore, developing an automated diagnostic system for retinopathy. He currently is a research associate at Schepens Eye Research Institute and an instructor at Harvard Medical School, working on HMD applications in low vision rehabilitation.

Noa Rensing is a senior scientist at MicroOptical Engineering Corporation. She is responsible for developing novel approaches to eyeglass displays and systems based on MicroOptical's eyeglass displays, and managing MicroOptical's low vision program. In addition, she performs in-house optical engineering tasks associated with the development, prototyping, and testing of new and existing optical systems, components, and procedures, and for working with the company's optical design consultants. She received her PhD in applied physics from Stanford University in 1995, studying the relationship between giant magnetoresistance and crystal structure in sputtered antiferromagnetically coupled multilayers. She received the BSc in both physics and mechanical engineering from M.I.T.
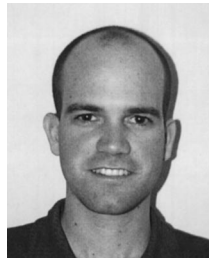
Evan Weststrate joined the MicroOptical Corporation in 2001. He has been responsible for all aspects of display electronics development including analog, microcontroller firmware, configurable logic, and system design. While studying for his MS in electrical engineering, he worked for the Tufts University Simulation Laboratory researching various techniques for simulating VLSI circuits. He has earned a BS in both mechanical and electrical engineering from Kettering University, and has worked as a manufacturing development engineer for Bose Corporation (Framingham, Massachusetts) and as an engineer for Engineered Plastic Components (Mattawan, Michigan).

Eli Peli received his BSEE, cum laude, and MSEE from the Technion-Israel Institute of Technology. He earned his doctorate from New England College of Optometry in Boston. He is a senior scientist and the Moakley scholar in aging eye research at the Schepens Eye Research Institute, and professor of ophthalmology at Harvard Medical School. He also serves on the faculty of the New England College of Optometry (adjunct professor of optometry and visual sciences). Since 1983 he has been caring for visually impaired patients as the director of the Vision Rehabilitation Service at the New England Medical Center Hospitals in Boston. He is a Fellow of the American Academy of Optometry, the Optical Society of America, and the Society for Information Display (SID). His principal research interests are image processing in relation to visual function and clinical psychophysics in low vision rehabilitation, image understanding, and evaluation of display-vision interaction.